



Effect of Pt, Pd, Au and Ag on oxidation behaviour of Fe₃Al intermetallic

G. Salinas, J. G. Gonzalez-Rodriguez, J. Porcayo-Calderon, V. M. Salinas-Bravo & G. Lara-Rodriguez

To cite this article: G. Salinas, J. G. Gonzalez-Rodriguez, J. Porcayo-Calderon, V. M. Salinas-Bravo & G. Lara-Rodriguez (2016) Effect of Pt, Pd, Au and Ag on oxidation behaviour of Fe₃Al intermetallic, Corrosion Engineering, Science and Technology, 51:3, 179-186, DOI: [10.1179/1743278215Y.0000000045](https://doi.org/10.1179/1743278215Y.0000000045)

To link to this article: <http://dx.doi.org/10.1179/1743278215Y.0000000045>



Published online: 18 May 2016.



Submit your article to this journal [↗](#)



Article views: 68



View related articles [↗](#)



View Crossmark data [↗](#)

Effect of Pt, Pd, Au and Ag on oxidation behaviour of Fe₃Al intermetallic

G. Salinas¹, J. G. Gonzalez-Rodriguez*¹, J. Porcayo-Calderon¹, V. M. Salinas-Bravo² and G. Lara-Rodriguez³

A study on the effect of the addition of 1 at-% noble elements such as Pt, Pd, Ag and Au on the oxidation resistance of Fe₃Al intermetallic alloy has been carried out at 900, 1000 and 1100°C during 100 h. For comparison, the same tests were performed on a Ni-base alloy type Inconel 600. At all the tested temperatures, parabolic growth rate was observed for the different alloys. The effect of the different noble elements was not unique at the different tested temperature. Thus, at 900°C, addition of Ag increased the mass gain, whereas Pd decreased it; at 1000°C, however, the opposite was true. At 1100°C, the mass gain was decreased by adding Pt, but Pd was very detrimental. In most of the cases, the scales were predominantly formed by Al₂O₃ with minor amounts of Fe₂O₃. Scale spallation was found when the noble elements were randomly distributed on the surface, but when they were finely distributed, the scale did not spall. In all cases, the mass gain for Fe₃Al alloy was lower than Inconel 600 type alloy.

Keywords: Intermetallic, Oxidation, Noble elements

Introduction

As candidates to be used in high temperature regimes, iron aluminides such as FeAl and Fe₃Al have received a lot of attention in the last few years.^{1,2} This is because they possess high creep resistance, low cost, high specific strength, low density, as well as high temperature oxidation and sulphidation resistance.^{3–5} Additionally, they have a notable high resistance to molten glasses,⁶ carburising gas mixtures⁷ and chlorine containing vapours.^{8,9} This good resistance of iron aluminides is due to the formation of a dense, adherent α -Al₂O₃ layer preceded by the formation of iron oxides and meta-stables γ -, δ - and θ -Al₂O₃, which grow faster and are more voluminous than α -Al₂O₃.^{10–13} However, there are barriers that limit the wide usage of binary alloys at room temperatures, which are their low ductility.^{14,15} A great deal of research work has been directed towards improving these properties, e.g. by adding alloying elements and by developing suitable thermomechanical treatments and forming techniques. One potential way to overcome these problems is the addition of alloying elements to the binary alloys. However, these additional chemical elements will affect the alloy oxidation resistance. For instance, Xu and Gao¹⁶ studied the effect of Zr and Y on the cyclic oxidation resistance of FeAl alloy at 1000–1200°C and found that their

additions, between 0.1 and 0.9 at-%, greatly increased the oxide spallation resistance. Janda *et al.*¹⁷ studied the effect of microalloying with Zr, Nb, C and B (0.5 at-%) on the oxidation behaviour of Fe₃Al and FeAl alloys at 750, 900 and 1050°C. Generally, as expected, an outstanding oxidation resistance of all investigated alloys was observed due to the formation of Al₂O₃ scales with a very slow growth rate. However, in contrast to binary iron aluminides in the same composition range, the mass gain with time increased with increasing aluminium content. Novák *et al.*¹⁸ studied the effect of Si on the oxidation behaviour of Fe–Al–Si alloys at 800°C in air. The Si content was between 5 and 30 wt-%. Tested alloys exhibited excellent oxidation resistance, which increased with silicon content up to 20 wt-%.

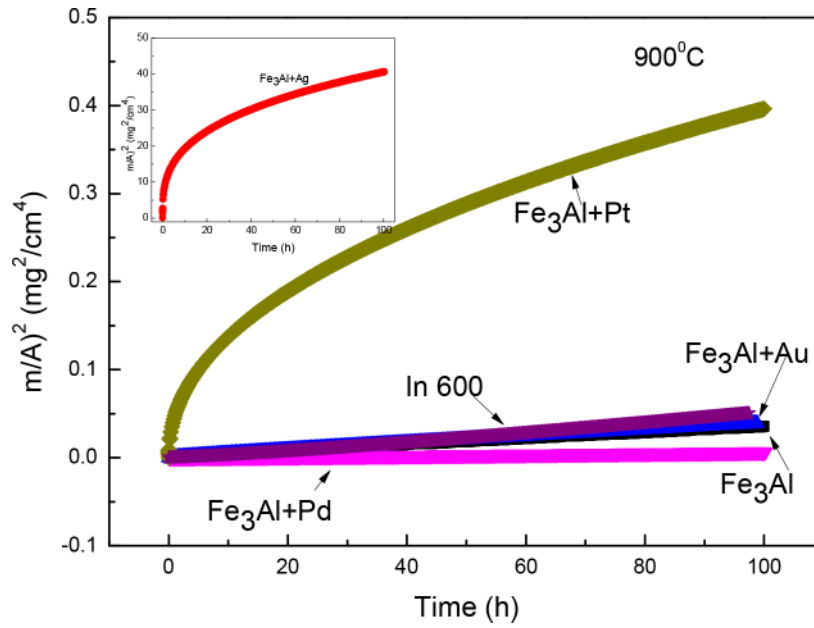
It is very well known that noble elements such as Ag, Au and Pt can form cathodic sites when added as alloying elements to engineering structural materials, but there is very little information regarding their effects on the corrosion performance of engineering materials in molten salts. Regarding the low temperature corrosion, the effect of noble elements when added to stainless steels in sulphuric acid, Peled and Itzhak¹⁹ found that additions of Ag improve the corrosion resistance and remains as inclusions, whereas additions of up to 2 wt-% were sufficient to preserve the passive state, but higher contents result in a high tendency for breakdown of the passive layer due to very high cathodic activity when Ag, Au, Pd and Pt were added.²⁰ With respect to the molten salt corrosion, Janz *et al.*^{21,22} evaluated the corrosion of gold–palladium, nickel, platinum, silver, gold and 347 type stainless steel in molten alkali carbonates at 600–900°C, finding little or negligible corrosion of noble elements, whereas 347 type stainless steel was found highly resistant to attack. Some other researchers have

¹Universidad Autonoma del Estado de Morelos, CIICAp, Av. Universidad 1001, Col. Chamilpa, 62500-Cuernavaca, Mor., Mexico

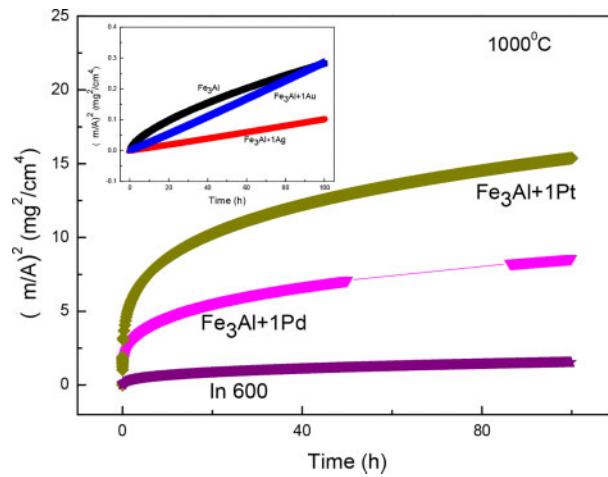
²I.I.E., Gerencia de Procesos Termicos, Av. Reforma 120, Temixco, Mor., Mexico

³Universidad Nacional Autonoma de Mexico, Instituto de Investigaciones en Materiales, Circuito Exterior S/N, Cd. Universitaria, Mexico DF C.P. 04510, Mexico

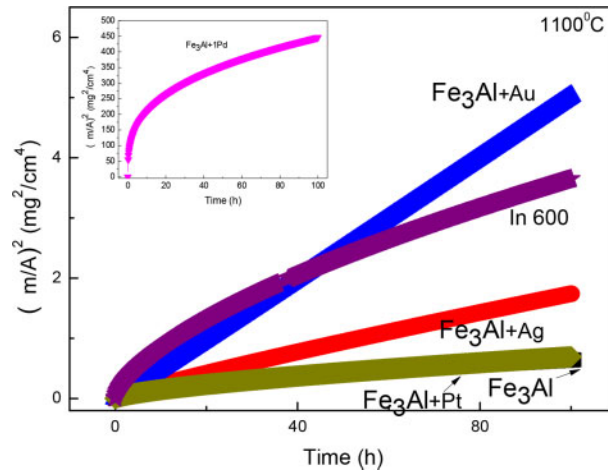
*Corresponding author, email ggonzalez@uaem.mx



1 Squared mass gain versus exposure time for Fe₃Al intermetallic alloy with additions of Au, Ag, Ti and Pt at 900°C



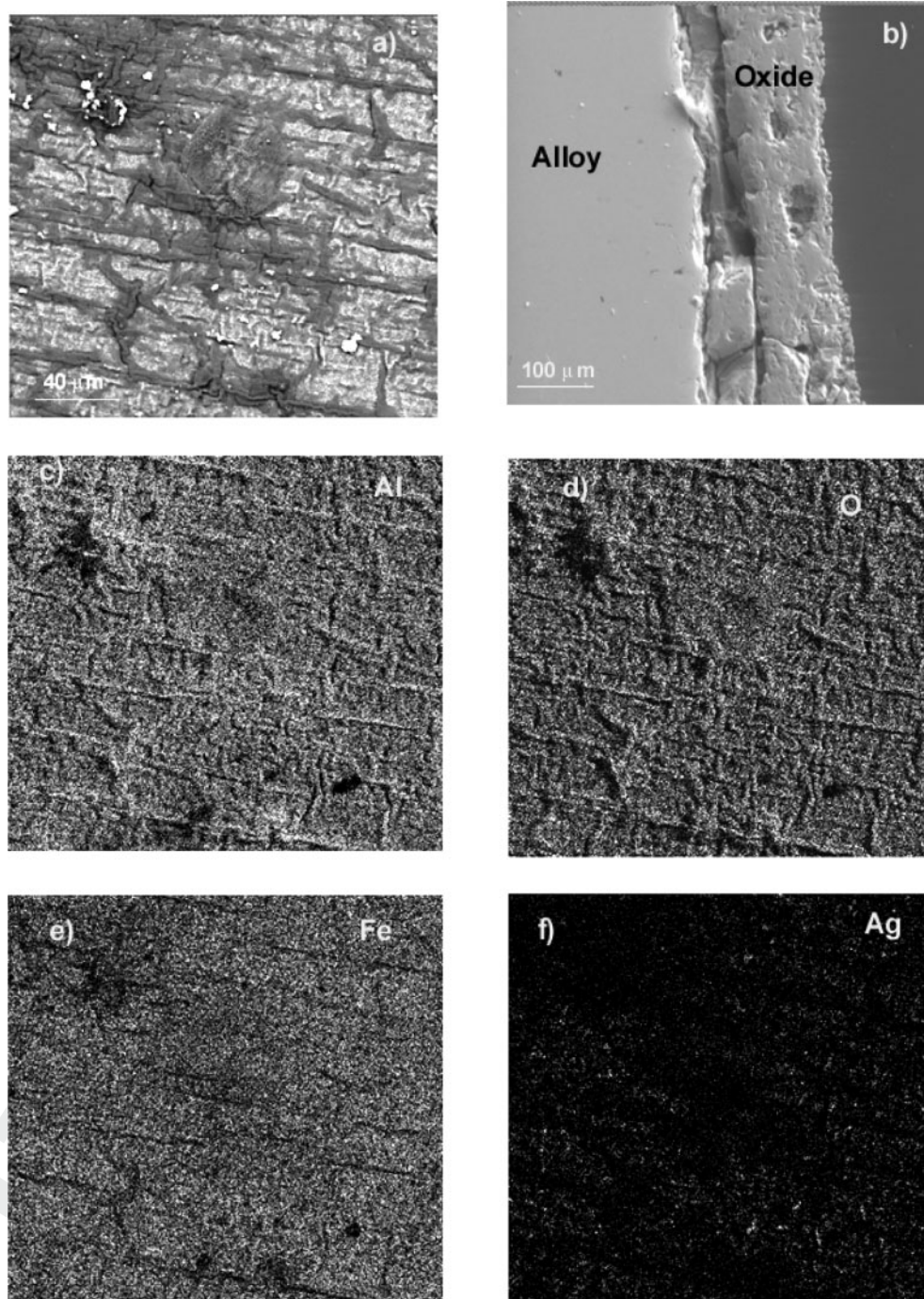
2 Squared mass gain versus exposure time for Fe₃Al intermetallic alloy with additions of Au, Ag, Ti and Pt at 1000°C

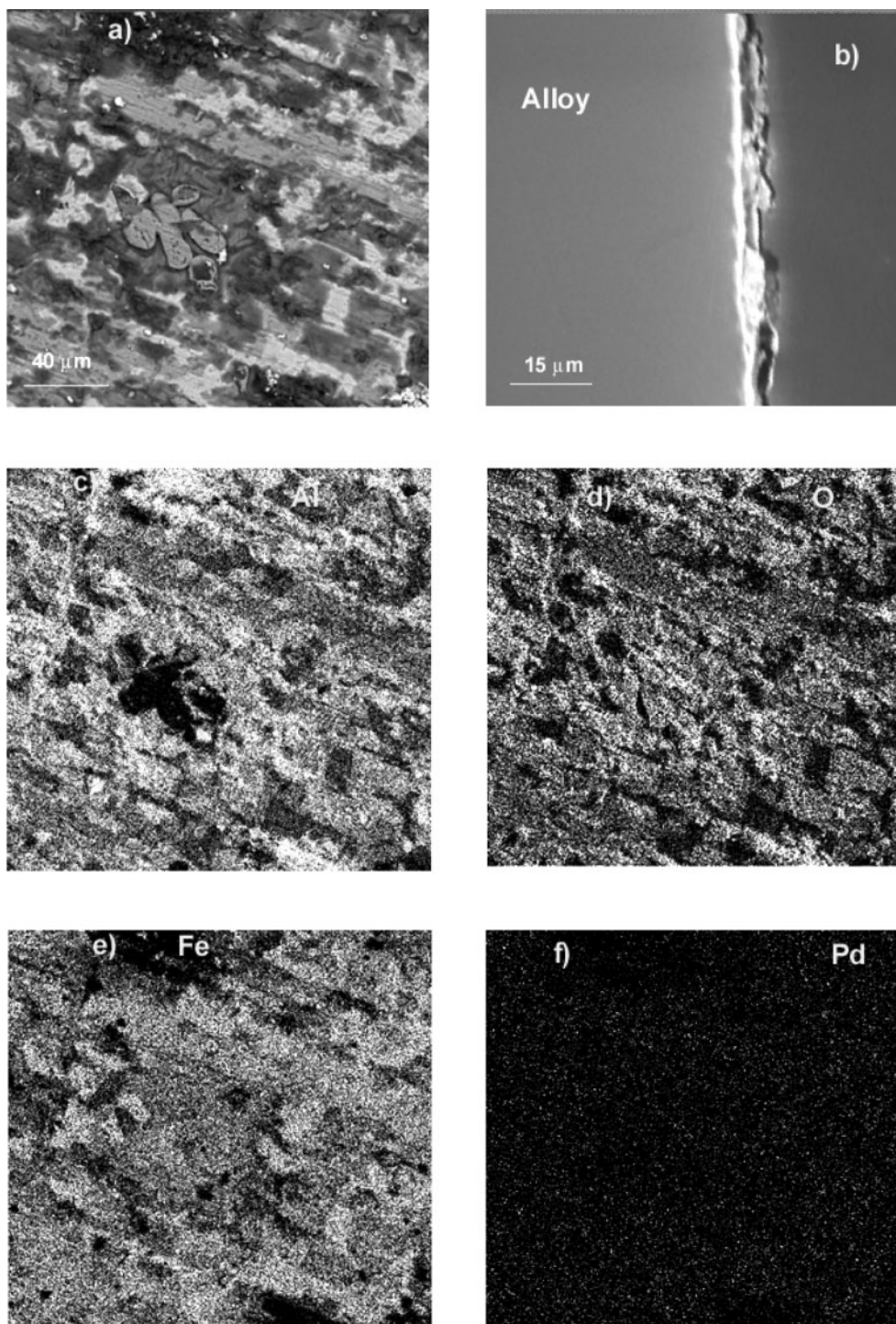


3 Effect of Au, Ag, Ti and Pt on squared mass gain versus exposure time for Fe₃Al intermetallic alloy at 1100°C

Table 1 Apparent parabolic rate constant k_p for different Fe₃Al intermetallic and Inconel 600 alloys

Alloy	$k_p, \text{g}^2/\text{cm}^{-4} \text{s}^{-1}$		
	900°C	1000°C	1100°C
Fe ₃ Al	3.57 E-14	1.86 E-13	2.79 E-13
Fe ₃ Al + 1Au	3.77 E-14	7.68 E-14	5.08 E-13
Fe ₃ Al + 1Ag	4.82 E-12	4.49 E-14	2.88 E-13
Fe ₃ Al + 1Pt	3.49 E-13	3.51 E-12	2.80 E-13
Fe ₃ Al + 1Pd	1.13 E-14	2.49 E-12	1.58 E-12
In 600	2.21 E-14	7.37 E-13	8.22 E-13

**4** SEM images of oxidised surface of Fe₃Al-Ag at 900°C showing *a* top view and *b* cross-section, together with X-ray mappings of *c* Al, *d* O, *e* Fe and *f* Ag



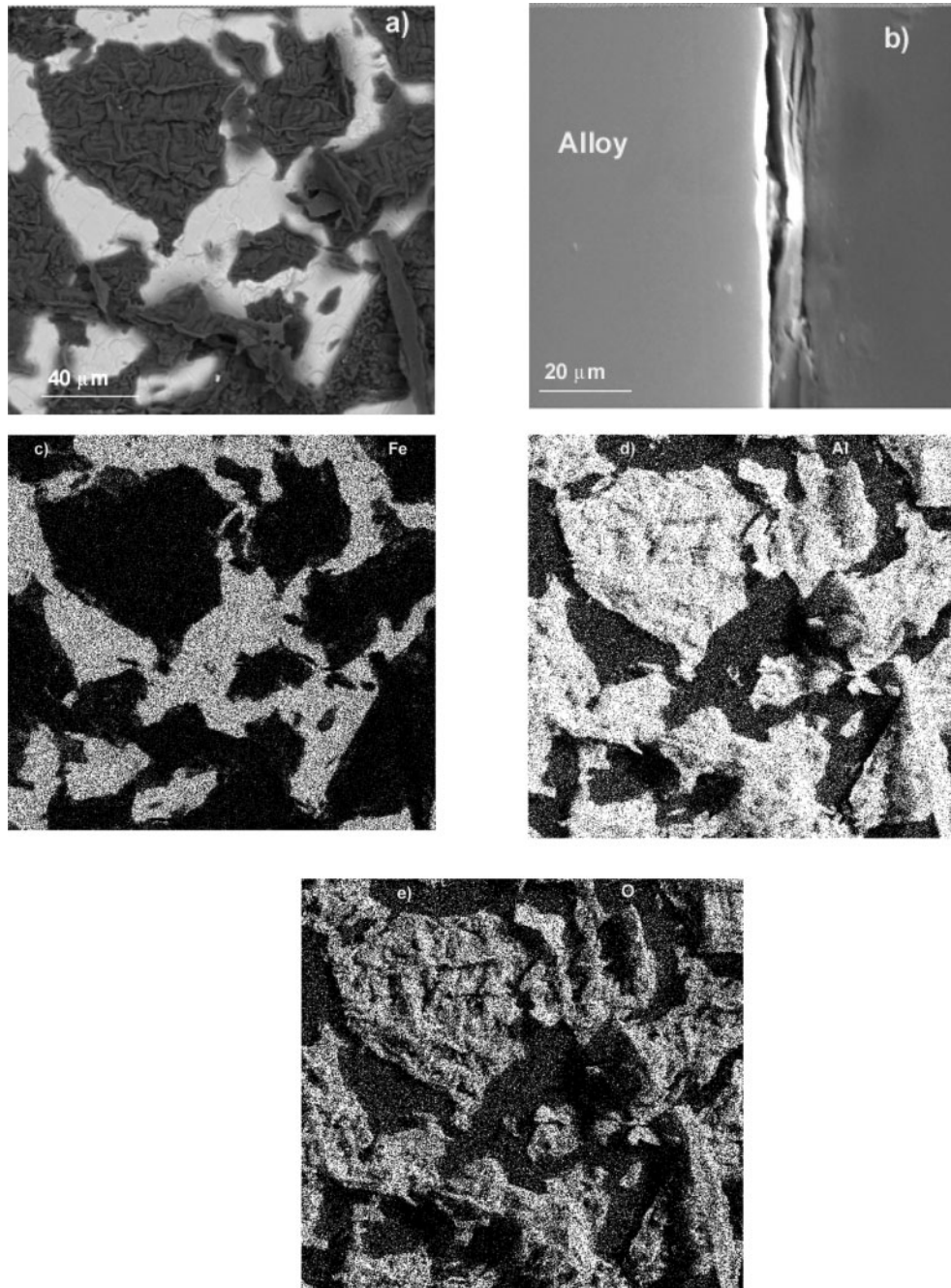
5 SEM images of oxidised surface of Fe₃Al–Pd at 900°C showing *a* top view and *b* cross-section, together with X-ray mappings of *c* Al, *d* O, *e* Fe and *f* Pd

studied the effect of noble elements in the oxidation behaviour²³ or sulphidation performance of structural materials such as Ni–Cr alloys^{24–29} but not on iron intermetallics. Thus, the aim of the present work is to study the effect of noble elements in the oxidation behaviour of Fe₃Al intermetallic in oxygen.

Experimental

Materials tested in this work include Fe₃Al with addition of 1 at-% Ag, Au, Pd or Pt. Intermetallic alloys with a nominal composition of Fe + 24Al + 1M, where M = Ag, Au, Pd

and Pt, were melted in an induction furnace using quartz crucibles under an argon atmosphere. All elements were 99.9% of purity. Specimens measuring 10 mm length × 5 mm height × 3 mm thick were prepared by grinding them to 1200 grade emery paper. Weight gain experiments were performed in pure oxygen at 900, 1000 and 1100°C in a thermobalance controlled via a desktop computer during 100 h. For comparison, the same tests under the same experimental conditions were performed using an Inconel 600 alloy containing Ni–8.26 wt-% Fe–17.20 Cr–0.49 Si. After oxidation tests, one of each specimen was mounted in bakelite in cross-section and polished



6 SEM images of oxidised surface of Fe₃Al at 1000°C showing *a* top view and *b* cross-section, together with X-ray mappings of *c* Fe, *d* Al and *e* O

to analyse the subsurface attack using a scanning electron microscopy (SEM) aided with energy dispersive spectroscopy to carry out microchemical analysis.

Results and discussion

The dependence of the squared mass gain during the oxidation of Fe₃Al alloys at 900, 1000 and 1100°C is shown in Figs. 1–3 respectively. It can be seen that these figures show a parabolic rate law at the different testing temperatures, with a fast mass gain at the beginning of the experiments during ~20 h, which is attributed to the fast growth of γ -, δ - and θ -Al₂O₃ metastable phases, which grow faster and are more voluminous than α -

Al₂O₃, although they were not detected in this work but have been reported in the literature.^{10–13} It can also be seen that the mass gain increased with the temperature, without any evidence of spallation, since the curves did not have any mass loss, indicating the good adherence of the formed scales. The effect of the different alloying elements was not very clear at the different testing temperatures. Thus, at 900°C, practically all the alloying elements except Pd increased the growth rate, being the alloy with the addition of Ag the one that showed the highest mass gain, whereas the lowest oxidation rate was obtained when Pd was added. Ni-base superalloy, Inconel 600, showed a very similar mass gain to that shown by the base, unalloyed Fe₃Al intermetallic alloy.

Parabolic rate constants, k_p , were obtained from the parabolic rate law

$$(\Delta m/A)^2 = k_p t \quad (1)$$

where $\Delta m/A$ is the mass gain per unit area (mg/cm^2) and listed in Table 1 confirmed this behaviour: the highest k_p value was for the alloy containing Ag, whereas the lowest k_p value was for the alloy containing Pd, very similar to that value obtained for Inconel 600 and Fe₃Al alloys.

On the other hand, at 1000°C (Fig. 2), the highest mass gain was for the alloy containing Ag, whereas the second highest was for the alloy containing Pd. The opposite behaviour was observed at 900°C. The addition of Au slightly decreased the mass gain of Fe₃Al intermetallic, which showed a mass gain much lower than that for Inconel 600. The values for k_p shown in Table 1 indicated this behaviour, with the highest k_p value for the alloy containing Ag, similar to its mass gain, whereas the highest value was obtained for the alloys containing Au and Ag. Finally, at 1100°C (Fig. 3), the addition of all the alloying elements, except Pt, increased the mass gain of base, unalloyed Fe₃Al intermetallic alloy, obtaining the highest mass gain, for more than two orders of magnitude, with the alloy containing Pd. The lowest mass gain was for the base, unalloyed Fe₃Al alloy and the one containing Pt, showing virtually the same mass gain values. Generally speaking, Table 1 shows an increase in the k_p value as the temperature increases, which is related with the accelerated diffusion of the oxide forming components with increasing the temperature.

Scale formed on Fe₃Al + Ag intermetallic alloy at 900°C (Fig. 4) consisted of a double, 150 μm thick layer, with an Al₂O₃ layer on top of an inner Fe₂O₃ as it has been reported in the literature.^{18,26,27} It can be seen in Fig. 4 that the oxide layer has been cracked, probably during cooling, precisely along the places where Ag particles can be seen in the sites where the scale has been cracked. The oxide had a flat shape and not needles, characteristic of the fast growing, voluminous, porous, non-protective θ -Al₂O₃, which grows at temperatures <900°C, whereas the flat shaped corresponds to the slow growing, protective α -Al₂O₃,¹⁷ which is stable at temperatures higher than 900°C. It has been reported that both Al₂O₃ and Fe₂O₃ are formed by the outward diffusion of Al and Fe ions. In the α -Al₂O₃, the diffusion is solely grain boundary and volume diffusion, much slower than in θ -Al₂O₃, which is a faster surface diffusion.¹⁷

It has been shown that for Ni-base superalloys, the formation of Ta rich particles at the metal/scale interface leads to spallation of the scales.^{29,30} One mechanism that leads to spallation is that Ag rich particles at the sample surface are undercut by the growing scale, which cracks at the particle/oxide interface during cooling.³⁰ On the other hand, for the alloy containing Pd (Fig. 5), the oxide scale was much thinner, only 10 μm thick, formed mainly by flat shaped α -Al₂O₃ and Fe₂O₃, without evidence of spalling or θ -Al₂O₃, since no needles shaped whiskers were found, may be due to the fact that Pd particles were finely distributed along the surface alloy, avoiding to be undercut by the slow growing oxide, as indicated by Fig. 1, which indicates that this alloy

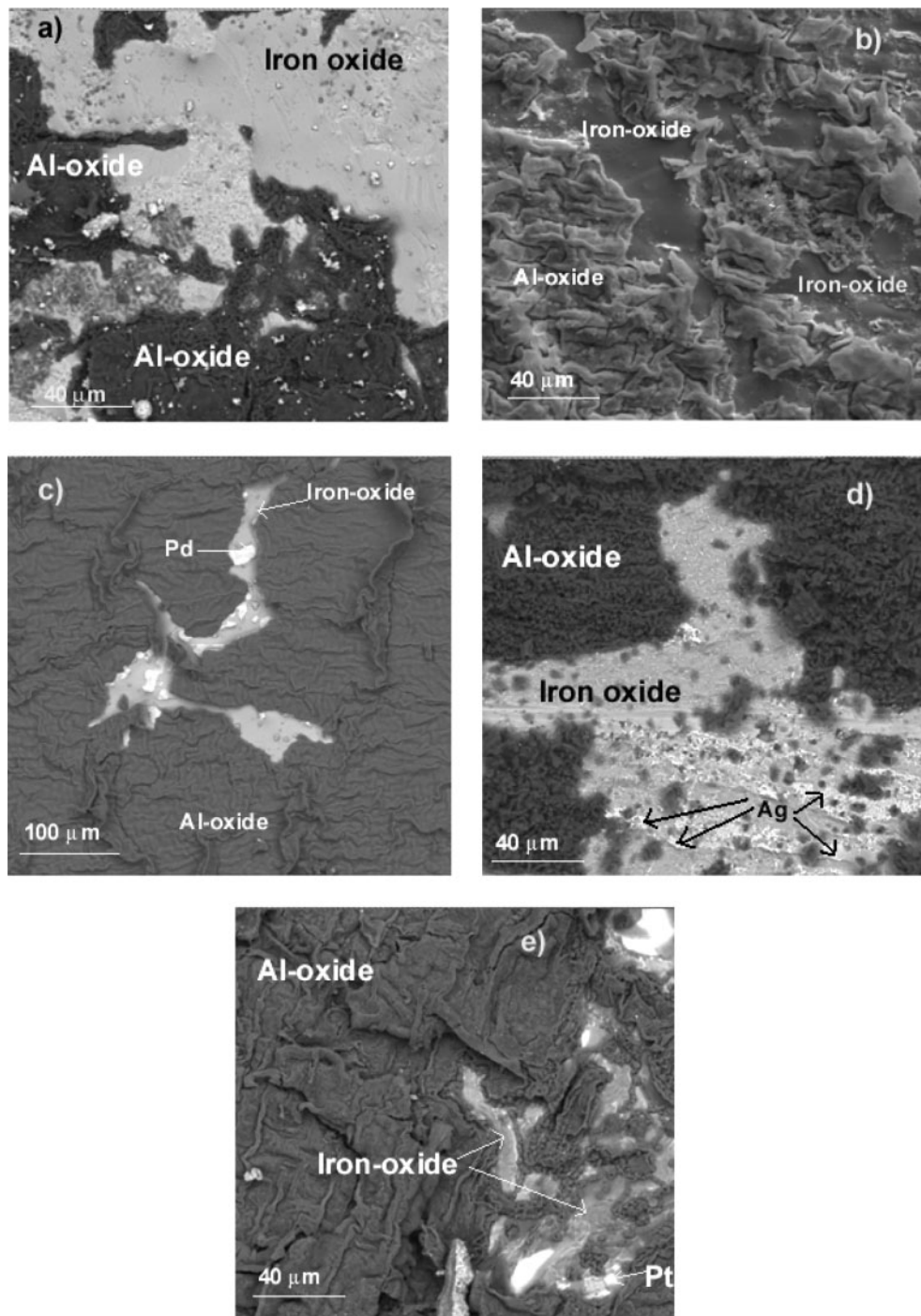
avoiding to be undercut by the slow growing oxide, as indicated by Fig. 1, which indicates that this alloy showed the lowest oxide growth rate. Additionally, Pint et al. showed that the presence of so called reactive elements like Zr or Y inhibits the outward diffusion of aluminium through the oxide scale and promotes the inward diffusion of oxygen, which thereby reduces the oxidation rate in NiAl and FeAl alloys.²⁹ This effect is attributed to the segregation of the reactive elements to grain boundaries in the oxide scale.²⁹ A similar role could be attributed to Pd in this case.

At 1000°C (Fig. 6), base Fe₃Al intermetallic, one of the alloys that exhibited a low mass gain, had a thin scale, ~10 μm thick, partially convoluted, which is made mainly of Al₂O₃ on top, and underneath of it iron oxide, probably Fe₂O₃. It can be seen that the Al₂O₃ layer has been cracked, probably during cooling, because the mass gain plots (Fig. 2) did not show any evidence of scale spalling. As has been described for binary Fe–Al³¹ and Fe–28Al–5 Cr,³² the iron oxide may have been formed in the initial stages of the oxidation. Unlike this, alloy containing Pt, which exhibited the highest mass gain value, exhibited a 100 μm thick, adherent oxide layer, but this time the Fe₂O₃ layer was on top of the Al₂O₃ scale, without evidence of Pt particles undercut by the growing oxide. These fast growing, no protective Fe₂O₃ and Al₂O₃ scales led to a parabolic growth of the scale during the test as it has been reported in other studies on the oxidation of Fe–Al alloys.^{10–13,28,29}

Finally, at 1100°C, none of the alloys exhibited protective scales, as can be seen in Fig. 7. For instance, unalloyed base Fe₃Al alloy (Fig. 7a) exhibited only Al₂O₃ underneath an Fe₂O₃ scale, with only a few cracks, which allowed it to have been one of the two alloys, together with the one containing Pt, with the lowest oxide growth rate, even lower than the Ni-base superalloy Inconel 600. On the other hand, the alloy containing Au, one of the alloys with the highest oxide growth rate, exhibited a convoluted, cracked Al₂O₃ layer, together with an Fe₂O₃ layer. For the alloy with the highest oxide growth rate, the alloy containing Pd (Fig. 7c) again, a convoluted, cracked Al₂O₃, together with minor amounts of Fe₂O₃ oxides, was found. In addition to this, some Pd particles were found, which caused the cracking of the scale, since, as explained above, these particles are undercut by the growing scale that cracks at the particle/oxide interface during cooling.³⁰ Similar to this, alloy containing Ag or Pt exhibited a convoluted, cracked, Al₂O₃ oxide with minor amounts of Fe₂O₃, with Ag or Pt particles respectively (Fig. 7d and e).

Conclusions

The effect of the addition of Pt, Pd, Ag and Au on the oxidation resistance of Fe₃Al intermetallic alloy at 900, 1000 and 1100°C during 100 h has been studied. It was found that at all the tested temperatures, parabolic growth rate was observed for the different alloys. However, the different elements had a different effect at the different testing temperatures. Thus, at 900°C, addition of Ag increased the mass gain but decreased it at 1000°C. The addition of Pd decreased the mass gain at 900°C but increased it at 1000°C. At 1100°C, the mass gain was decreased by adding Pt, but Pd was very det-



8 SEM images of oxidised surfaces of a Fe₃Al, b Fe₃Al–Au, c Fe₃Al–Pd, d Fe₃Al–Ag and e Fe₃Al–Pt alloys at 1100°C

rimental. Scales were predominantly formed by Al₂O₃ with minor amounts of Fe₂O₃. When the noble elements were randomly distributed on the surface, scale spallation was found, but when they were finely distributed, the scale did not spall.

References

1. P. F. Tortorelli and K. Natesan: 'Critical factors affecting the high temperature corrosion performance of iron aluminides', *Mater. Sci. Eng. A*, 1998, **258**, 115–125.
2. J. Klöwer, U. Brill and U. Heubner: 'High temperature corrosion behaviour of nickel aluminides: effects of chromium and zirconium', *Intermetallics*, 1999, **7**, 1183–1194.
3. N. Babu, R. Balasubramaniam and A. Ghosh: 'High-temperature oxidation of Fe₃Al-based iron aluminides in oxygen', *Corros. Sci.*, 2001, **43**, 2239–2254.
4. P. Hausild, M. Karlik, T. Skiba, P. Sajdl, J. Dubský and M. Palm: 'High temperature oxidation of spark plasma sintered and thermally sprayed FeAl-based iron aluminides', *Acta Phys. Pol. A*, 2012, **122**, 545–551.
5. X. Zhu, Z. Yao, X. Gu, W. Cong and P. Zhang: 'Microstructure and corrosion resistance of Fe–Al intermetallic coating on 45 steel synthesized by double glow plasma surface alloying technology', *Trans. Nonferrous Met. Soc. China*, 2009, **19**, 143–148.
6. V. Šíma, P. Kratochvíl, P. Kozelský, I. Schindler and P. Hána: 'FeAl-based alloys cast in an ultrasound field', *Int. J. Mater. Res.*, 2009, **100**, 382–385.
7. P. Kratochvíl, F. Dobes and V. Vodicková: 'The effect of silicon on the structure of Fe–40 at.% Al type alloys with high contents of carbon (1.9–3.8 at.%)', *Intermetallics*, 2009, **17**, 39–45.
8. P. Kratochvíl: 'The history of the search and use of heat resistant Pyroferal alloys based on FeAl', *Intermetallics*, 2008, **16**, 587–591.
9. G. H. Meier and F. S. Pettit: 'High temperature oxidation and corrosion of intermetallic compounds', *Mat. Sci. Technol.*, 1992, **8**, 331–338.

10. M. Kupka: 'Technological plasticity studies of the FeAl intermetallic phase based alloy', *Intermetallics*, 2004, **12**, 295–302.
11. K. Wolski, F. Thévenot and J. Le Coze: 'Effect of nanometric oxide dispersion on creep resistance of ODS-FeAl prepared by mechanical alloying', *Intermetallics*, 1996, **4**, 299–307.
12. H. J. Grabke, M. Brumm and M. Steinhorst: 'Development of oxidation resistant high temperature intermetallics', *Mater. Sci. Technol.*, 1992, **8**, 339–344.
13. T. Skiba, P. Hausild, M. Karlík, K. Vanmeensel and J. Vleugels: 'Mechanical properties of spark plasma sintered FeAl intermetallics', *Intermetallics*, 2010, **18**, 1410–1414.
14. A. Barnoush, J. Dake, N. Kheradmand and H. Vehoff: 'Examination of hydrogen embrittlement in FeAl by means of in situ electrochemical micropillar compression and nanoindentation techniques', *Intermetallics*, 2010, **18**, 1385–1389.
15. A. Barnoush, M. Zamanzade, H. Vehoff and A. Barnoush: 'Direct observation of hydrogen-enhanced plasticity in super duplex stainless steel by means of in situ electrochemical methods', *Scr. Mater.*, 2010, **62**, 242–245.
16. C. H. Xu and W. Gao: 'Oxidation behaviour of FeAl intermetallics: effects of reactive elements on cyclic oxidation properties', *Mater. Sci. Technol.*, 2001, **17**, 324–332.
17. D. Janda, H. Fietzek, M. Galetz and M. Heilmaier: 'The effect of micro-alloying with Zr and Nb on the oxidation behavior of Fe₃Al and FeAl alloys', *Intermetallics*, 2013, **41**, 51–57.
18. P. Novák, M. Zelinková, J. Serák, A. Michalcová, M. Novák and D. Vojtech: 'Oxidation resistance of SHS Fe-Al-Si alloys at 800 °C in air', *Intermetallics*, 2011, **19**, 1306–1312.
19. P. Peled and D. Itzhak: 'The effect of noble alloying elements Ag, Pt and Au on the corrosion behavior of sintered stainless steel in an H₂SO₄ environment', *Corros. Sci.*, 1988, **28**, 1019–1028.
20. P. Peled and D. Itzhak: 'The surface composition of sintered stainless steel containing noble alloying elements exposed to a H₂SO₄ environment', *Corros. Sci.*, 1991, **32**, 83–90.
21. G. J. Janz, A. Conte and E. Neuenschwander: 'Corrosion of platinum, gold, silver and refractories in molten carbonates', *Corrosion*, 1963, **19**, 2921–2941.
22. G. J. Janz and A. Conte: 'Corrosion of gold–palladium, nickel and type 347 stainless steel in molten carbonates', *Corrosion*, 1964, **20**, 237t–238t.
23. Y. Niu, Z. L. Zhao, F. Gesmundo and M. Al-Omary: 'The air oxidation of two Cu-Ni-Ag alloys at 600–700°C', *Corros. Sci.*, 2001, **43**, 1541–1556.
24. X. X. Ma, Y. D. He and D. R. Wang: 'Inert anode composed of Ni-Cr alloy substrate, intermediate oxide film and α -Al₂O₃/Au (Au-Pt, Au-Pd, Au-Rh) surface composite coating for aluminum electrolysis', *Corros. Sci.*, 2011, **53**, 1009–1017.
25. G. Wang, R. Carter and D. L. Douglass: 'High temperature sulfidation of Fe-Nb alloys', *Oxid. Met.*, 1989, **32**, 273–294.
26. R. Shiring and D. L. Douglass: 'Sulfidation behavior of rhenium and cobalt-rhenium alloys', *Oxid. Met.*, 1999, **52**, 353–377.
27. D. Janda, H. Fietzek, M. Galetz and M. Heilmaier: 'The effect of micro-alloying with Zr and Nb on the oxidation behavior of Fe₃Al and FeAl alloys', *Intermetallics*, 2013, **41**, 51–57.
28. A. Hotar and M. Palm: 'Oxidation resistance of Fe-25Al-2Ta (at.%) in air', *Intermetallics*, 2010, **18**, 1390–1395.
29. B. A. Pint, I. G. Wright, W. Y. Lee, Y. Zhang, K. Prüßner and K. B. Alexander: 'Substrate and bond coat compositions: factors affecting alumina scale adhesion', *Mater. Sci. Eng.*, 1998, **A245**, 201–211.
30. I. G. Wright, B. A. Pint, W. Y. Lee, K. B. Alexander and K. Prüßner: 'Some effects of metallic substrate composition on degradation of thermal barrier coatings', in 'High temperature surface engineering', (ed. J. Nicholls and D. Rickerby), 95–113; 2000, London, Institute of Materials.
31. B. Pöter, F. Stein, R. Wirth and M. Spiegel: 'Early stages of protective oxide layer growth of binary iron aluminides', *Z. Phys. Chem.*, 2005, **219**, 1489–1503.
32. P. F. Tortorelli and J. H. DeVan: 'Behavior of iron aluminides in oxidizing and oxidizing/sulfidizing environments', *Mater. Sci. Eng.*, 1992, **A153**, 573–560.